Parameter Estimation Algorithm for a PEM Electrolyzer Equivalent Circuit Model Under Current Ripple Conditions

Ángel Hernández-Gómez, Diego Langarica-Cordoba, Panfilo R. Martinez-Rodriguez, Hernán González-Aguilar, Damien Guilbert, Belem Saldivar

***Abstract*—Unknown parameter estimation for electrical models of proton exchange membrane (PEM) electrolyzers is important for optimal hydrogen production and storage in power systems. Algorithms for correctly identifying parameters for different models, including equivalent circuit models (ECM), have been reported. These are important for analyzing the transient dynamics of the PEM electrolyzer connected to grid-tied power electronics sources. However, no method has been reported to correctly estimate the ECM parameters when subjected to current ripple from power electronics. Current ripple is an important issue requiring further investigations since they are responsible for the accelerated aging of electrolyzers. In this work, an algorithm has been developed to estimate the parameters of an ECM for the electrolyzer voltage under input current ripple. Furthermore, based on the gradient method, this algorithm allows adapting the parameters with the values of the proposed electronic components, i.e., resistors, capacitors, and voltage sources. The proposed algorithm has been validated using two voltage-current databases obtained from a commercial PEM electrolyzer system NMH2 1000. Thus, by efficiently estimating the ECM parameters, the proposed algorithm facilitates the design and construction of power converters coupled to the electrolyzer under current ripple constraints.**

***Keywords*—PEM electrolyzer; Electrolyzer modeling; Equivalent circuit model; Parameter estimator.**

I. Introduction

HYDROGEN is considered a key energy vector for energy transition purposes to meet climate-neutral by 2050 [1]. At present, most hydrogen is generated by employing thermochemical processes (steam methane reforming, coal gasification) that may be coupled with carbon capture, utilization, and storage solutions [2]. Over the last few years, many countries have adopted a strategy dedicated to the production and the use of low-carbon hydrogen obtained through a water electrolysis process fed by renewable energy sources (RES) [3]. Indeed, the water electrolysis process has reached commercial maturity as evidenced by numerous green hydrogen power plants developed worldwide [4]. The water electrolysis process consists of splitting pure water thanks to electricity into pure hydrogen and oxygen. Consequently, electrolyzers can convert surplus renewable energy into hydrogen, serving as an energy storage medium. The electrolysis is performed in different ways according to the type of electrolyte material employed and the ionic species they transport [5].

The electrolyzers can be classified into two categories: low-temperature electrolyzers (LTE) and high-temperature electrolyzers (HTE). Alkaline, proton exchange membrane (PEM), and anion exchange membrane (AEM) belong to the LTE category; while solid oxide (SO) to the HTE category [6]. Among these four different types of electrolyzers, only alkaline and PEM electrolyzers run the global market; while AEM and SO technologies, despite their recent introduction in the electrolyzer market, are still in-depth research and development to enhance their performance [7]. On one hand, alkaline electrolyzers offer the lowest investment cost and higher lifetime than the other electrolyzer technologies [8]. On the other hand, their alkaline liquid solution, mainly based on 25-30% of potassium hydroxide, requests frequent maintenance and limits their operational flexibility, i.e., 15-100% [5]. On the other side, PEM electrolyzers, despite their higher costs (use of platinum-group metals for the catalysts) and specific energy consumption, present an extended current density ($>3\ A \cdot cm^{-2}$) and larger operational flexibility (0-100%), making them particularly fit for their coupling with intermittent RES [9]. Due to its advantages, the PEM electrolyzer has been considered in this research work.

As pointed out in review papers [10], [11], modeling of PEM electrolyzer voltage under real operating conditions, static and dynamic considering intermittent RES, and operating variables, i.e., temperature and gas pressure, have become a pertinent research topic. Indeed, a better understanding of the real behaviors of PEM electrolyzers allows the development of accurate simulation tools, emulators, and the design of power converters including their controls [12]. On the other hand, the characterization and modeling of PEM electrolyzers supplied by currents including harmonics (low and high-frequency ripple) from power electronics have not been yet covered in the literature. Indeed, relying on the first outcomes reported in [13], triangular current ripple at 10 kHz from DC-DC converters has been identified as the most degrading condition, favoring

Á. Hernández-Gómez, D. Langarica-Cordoba, P. R. Martinez-Rodriguez and H. González-Aguilar are with the School of Sciences, Universidad Autónoma de San Luis Potosí (UASLP), San Luis Potosí, 78295, San Luis Potosí, Mexico (e-mails: angel.hernandez@uaslp.mx, diego.langarica@uaslp.mx, pamartinez@ieee.org, hernan@fc.uaslp.mx). D. Guilbert is with the Université Le Havre Normandie, GREAH, 76600 Le Havre, France (e-mail: damien.guilbert@univ-lehavre.fr). B. Saldivar is with Department of Automatic Control, CINVESTAV-IPN, Av. Instituto Politécnico Nacional 2508, Mexico City 07360, Mexico (e-mail: belem.saldivar@cinvestav.mx).

Paper submitted to the International Conference on Power Systems Transients (IPST 2025) in Guadalajara, Mexico, June 8-12, 2025.

consequently degradations, i.e., high-frequency resistance rise, corrosion, and titanium mesh. This aspect is particularly explored in this work for introducing a new research area to the current literature.

As reported, PEM electrolyzer models consist of different unknown parameters, and proper identification of these parameters is necessary for optimal performance [14]. Furthermore, since the PEM electrolyzer parameters vary depending on the operating conditions above-mentioned, algorithms must be developed to calculate these changing parameters [15]. In [16], the operating parameters of the PEM electrolyzer have been optimized to decrease the required input voltage using the Taguchi method. A thermodynamic model was developed, and the Taguchi method was applied to calculate the performance of the electrolyzer. The results in [16] showed the optimal conditions for temperature, membrane water content, current density, membrane thickness, cathode pressure, and anode pressure. The authors in [17] have calculated seven parameters of a PEM electrolyzer voltage model using the honey badger algorithm. The proposed method in [17] employs an objective function defined as the sum of the squared error between the experimental and the estimated voltage. Finally, the honey badger algorithm has been validated by comparing the experimental and estimated I-V curves using the calculated parameters. In [18], a method for parameter estimation of a PEM electrolyzer model with eight unknown model parameters has been proposed based on the modified honey badger algorithm. The precision of the proposed algorithm in [18] has been validated with polarization curves.

The equivalent circuit model (ECM) for PEM electrolyzer voltage has proven its importance in analyzing the electrolyzer's dynamic response when connected to intermittent renewable resources [19], [20]. Algorithms have been developed to estimate the model parameters, as well as the parameters of the electrochemical models [21]. In [15], the authors have developed a multi-innovation least squares identification algorithm to identify the ECM parameters for the PEM electrolyzer voltage. The proposed algorithm in [15] improves the convergence speed of numerical algorithms and avoids the local optimization problem present in heuristic algorithms. However, an algorithm to estimate the ECM parameters subjected to ripple data has not been reported. For this reason, the main contribution of this paper is to propose and validate a robust and easy-to-implement algorithm to estimate the parameters of an ECM considering supply currents with low and high-frequency ripple. Two sets of experimental data from a commercial PEM electrolyzer system, including its power electronics, are used to ensure the algorithm's good performance. The comparison between the simulations using the parameters obtained by the algorithm and the experimental data has revealed the ECM's utility in predicting the electrolyzer's real voltage response under current ripple constraints. This innovative algorithm is important for the investigation of the effects of the current ripple on the performance of the PEM electrolyzer. The correct estimation of ECM parameters improves the understanding of transient dynamics and enhances the design of power converters, ensuring efficient and stable operation under current ripple conditions.

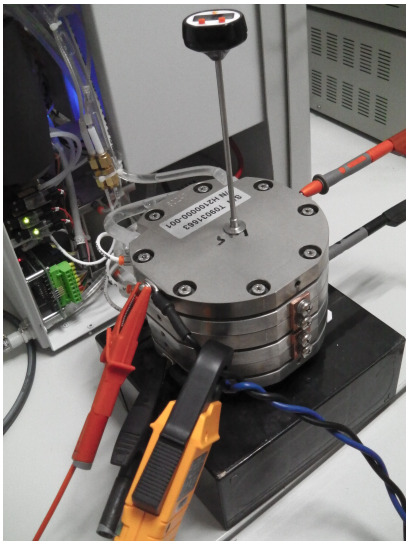

Fig. 1: PEM electrolyzer system used to obtain the experimental data.

TABLE I: Specifications of the PEM electrolyzer system NMH2 1000 from HELIOCENTRIS® Company.

Parameter	Value	Unit
Rated electrical power	400	W
Rated stack voltage	8	V
Stack current range	0-50	A
Hydrogen outlet pressure	10.5	bar
Cells number	3	-
Active area section	50	cm^2
Hydrogen flow rate range at STP	0-1	slpm

II. Experimental Test Setup and Data Collection

For the collection of experimental data, the commercial PEM electrolyzer system NMH2 1000 from HELIOCENTRIS® Company was utilized, see Figure 1. The specifications of this PEM electrolyzer are presented in Table I. In this PEM electrolyzer, the hydrogen flow rate at standard temperature (STP) and pressure, $15°C$ and 1 bar, respectively, are given in standard liter per minute (slpm). The generated hydrogen is stored in metal hydride storage tanks to offer high safety levels. Besides, the PEM electrolyzer stack is directly fed by pure water featuring low conductivity, i.e., less than 2 μScm^{-1}.

Given that the PEM electrolyzer system used in this work is commercial, it comprises power electronics to feed the electrolyzer as depicted in Figure 2. The main AC source in this case is the power grid (230 V/50 Hz) and the DC load is the PEM electrolyzer. The power electronics part includes a single-phase diode bridge rectifier, a DC-link capacitor, and a DC-DC converter. As presented in Table I, the PEM electrolyzer stack requests a very low DC voltage, i.e., 8 V at rated power. For this reason, a step-down DC-DC converter is used.

In this system, the single-phase diode bridge rectifier generates a low-frequency current ripple, i.e., 100 Hz, while

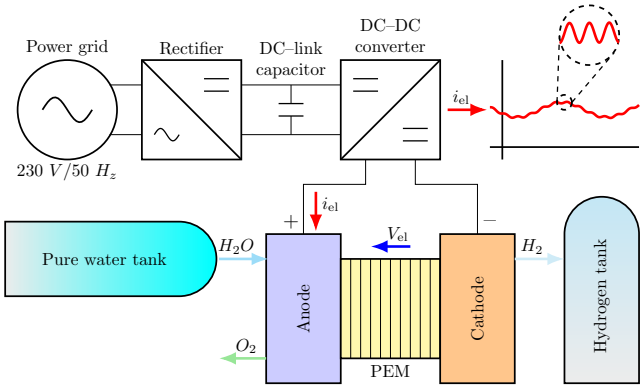

Fig. 2: PEM electrolyzer and hydrogen storage system, including grid-tied power electronics source.

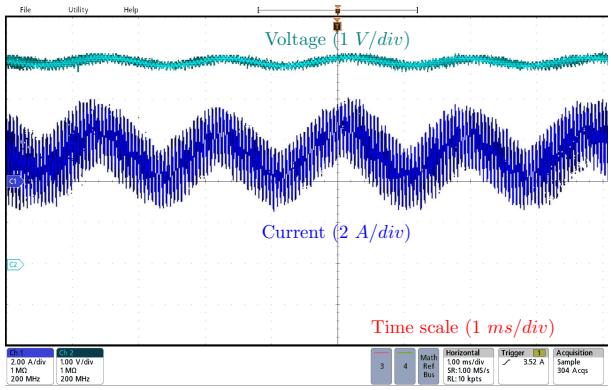

Fig. 3: Voltage-current oscilloscope screenshot from the first database, i_{el}=2 A.

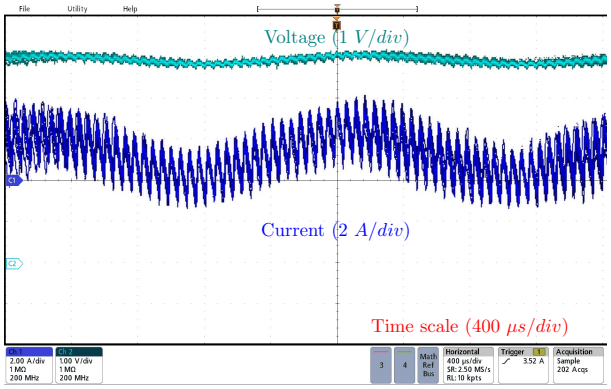

Fig. 4: Voltage-current oscilloscope screenshot with zoom from the first database.

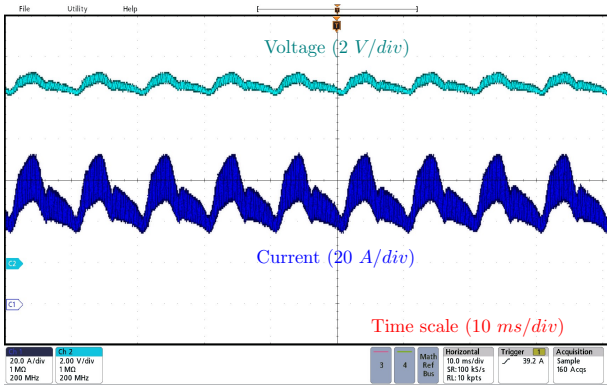

Fig. 5: Voltage-current oscilloscope screenshot from the second database, i_{el}=40 A.

the step-down DC-DC converter produces a high-frequency current ripple, i.e., 10 kHz. To meet the objectives of this work, two databases from the PEM electrolyzer, i.e., stack current i_{el} and voltage v_{el} are utilized. Stack current and voltage are acquired via the use of voltage and current probes, as shown in Figure 1. These data correspond to two different operating points, i_{el}=2 A and i_{el}=40 A, where the PEM electrolyzer system operates autonomously. These two operating points have not been chosen by the authors. Indeed, the used PEM electrolyzer can operate automatically, either at a low current (low hydrogen flow rate) or at a high current (to increase the hydrogen flow rate).

The obtained experimental results are represented in Figures 3 and 4 related both to the first operating point, i_{el}=2 A, and Figure 5 related to the second operating point, i_{el}=40 A. In Figure 3, the low-frequency AC component of the current can be observed, whereas in Figure 4 the high-frequency AC component can be stressed. For this first operating point, the current ripple constitutes 200%, i.e., 4 A of the average current value. Besides, a small AC component in the stack voltage response can be noticed, i.e., around 0.3 V. Regarding the second operating point, the current ripple represents 96%, i.e., 38 A of the average current value. Like in the first operating point case, a slight AC component can be perceived in the stack voltage response, approximately 1.26 V.

By comparing Figures 3 and 5, the voltage ripple for the second operating point is four times higher than the first operating point. It means that the current ripple is less mitigated, consequently affecting the electrolyzer's voltage response. In summary, the higher the current amplitude, the less the current ripple is mitigated by the electrolyzer's double layer capacitance phenomenon. Besides, as reported in the conclusions of the work of [22], a major concern is the maximum current allowable by the double-layer capacitance, making it possible to guarantee the mitigation of the current ripple. For this reason, further research is required to gain a better understanding of the link between the current ripple and the degradations of the electrolyzer. The outcomes of these investigations might be useful to design optimally a power converter avoiding likely degradations.

III. Mathematical Model and Algorithm

PEM electrolyzers, through ECM, can be modeled using different electronic components and combinations of resistance, capacitance, and voltage sources [4], [23]. Furthermore, in an ECM, complex systems can be simplified using physical properties and losses of these components [24], [25].

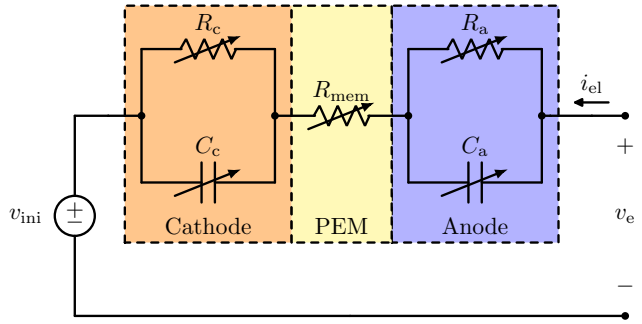

Fig. 6: Equivalent electronic circuit diagram for PEM electrolyzer voltage $v_e = v_{rev} + v_{act} + v_\Omega$.

A. ECM for the PEM electrolyzer voltage

This work estimates the parameters of the ECM developed in the works [26], [27]. In this ECM, the PEM electrolyzer voltage $v_e = v_{rev} + v_{act} + v_\Omega$ describes the reversible voltage v_{rev}, the activation voltage v_{act}, and the ohmic voltage v_Ω in terms of electrical components, i.e., one DC voltage source, two capacitors, and three resistors, see Figure 6. Based on the equivalent electronic circuit of Figure 6, the ECM is presented as follows:

- A DC voltage source v_{ini}. This voltage source is used to model the reversible voltage v_{rev}.
- A resistance R_{mem}. Usually, this resistance is used to model the electrolyzer membrane and also the contact resistances between the electrodes and the membrane. Thus, the ohmic voltage is calculated as $v_\Omega = R_{mem} \cdot i_{el}$, where i_{el} is the input current of the electrolyzer.
- Two resistor-capacitor branches. These branches are used to model the activation voltage $v_{act} = K \cdot (v_{act,c}, v_{act,a})^T$, one branch for the activation voltage in the cathode $v_{act,c}$ and the other branch for the activation voltage in the anode $v_{act,a}$. $K = (k_1, k_2)$ is a constant two-input vector that depends on the input current. In addition, as reported in the literature, the activation voltage is responsible for the dynamics present in the PEM electrolyzer voltage. The dynamic equations are defined as:

$$\frac{dv_{act,c}}{dt} = \frac{1}{C_c} i_{el} - \frac{1}{\tau_c} v_{act,c}, \tag{1}$$

$$\frac{dv_{act,a}}{dt} = \frac{1}{C_a} i_{el} - \frac{1}{\tau_a} v_{act,a}, \tag{2}$$

where C_c and C_a are the capacitors for the cathode and the anode, respectively. τ_c and τ_a are the electrical time constants that depend strongly on the operating conditions at the cathode and the anode, respectively. Furthermore, the resistances R_c (cathode) and R_a (anode) from the two resistor-capacitor branches vary depending on the current input and can be calculated using (3) and (4), as follows:

$$R_c = \frac{\tau_c}{C_c}, \tag{3}$$

$$R_a = \frac{\tau_a}{C_a}. \tag{4}$$

The differential equations (1) and (2) can be rewritten as a linear system.

$$\begin{pmatrix} \frac{dv_{act,c}}{dt} \\ \\ \frac{dv_{act,a}}{dt} \end{pmatrix} = A \cdot \begin{pmatrix} v_{act,c} \\ \\ v_{act,a} \end{pmatrix} + B \cdot i_{el}, \tag{5}$$

where

$$A = \begin{pmatrix} -\frac{1}{\tau_c} & 0 \\ \\ 0 & -\frac{1}{\tau_a} \end{pmatrix} \text{ and } B = \begin{pmatrix} \frac{1}{C_c} \\ \\ \frac{1}{C_a} \end{pmatrix}.$$

Thus, the ECM for the PEM electrolyzer voltage based on the equivalent electronic circuit of Figure 6 is expressed as:

$$v_e = v_{ini} + R_{mem} \cdot i_{el} + K \cdot (v_{act,c}, v_{act,a})^T. \tag{6}$$

Once the model is defined for estimation purposes, the array parameters A and B from (5) and the parameters v_{ini}, R_{mem}, and $K = (k_1, k_2)$ from (6) are estimated using the gradient method algorithm.

B. The gradient method algorithm

To apply the algorithm and calculate the parameters using the gradient method, it is noted that (6) can be expressed as a product of two vectors, a vector of parameters θ and a vector of time-dependent functions $\phi(t)$, as follows:

$$v_e = \theta \cdot \phi(t), \tag{7}$$

where

$$\theta = (v_{ini}, R_{mem}, k_1, k_2),$$

and

$$\phi(t) = (1, i_{el}, v_{act,c}, v_{act,a})^T.$$

Many parameter identification algorithms have been based on the gradient method because of its easy application, fast programming, and exponential convergence [28]. For (7), v_e and $\phi(t)$ are known signals and θ is unknown. The vector $\phi(t)$ is called the regressor vector and the standard linear error equation is defined as:

$$e = (\hat{\theta} - \theta) \cdot \phi(t), \tag{8}$$

where $\hat{\theta}$ is a vector of estimated parameters for θ. Therefore, the gradient algorithm builds an identifier structure using the signals of the regressor $\phi(t)$ and v_e taking into account (8). A differential equation defines the gradient algorithm, called the law of updating. In this work, the standard gradient algorithm is defined using the law of updating:

$$\dot{\hat{\theta}} = -g \cdot e \cdot \phi(t) \text{ with } g > 0. \tag{9}$$

The right-hand side of (9) is proportional to the gradient of the output error squared, viewed as a function of $\hat{\theta}$,

$$\frac{\partial}{\partial \hat{\theta}}(e^2) = 2e \cdot \phi(t). \tag{10}$$

Algorithm to calculate the parameters θ.

1: To collect and save experimental PEM electrolyzer voltage data resulting from an input current i_{el}. This input current must also be saved.
2: To define initial values for the resistors R_{c} and R_{a} and for the capacitors C_{c} and C_{a} to generate A and B of the system (5).
3: To develop a numerical method for solving the system (5) using the values obtained for the arrays A and B in the previous step and the initial value $v_{\mathrm{act}}(0)$.
4: To complete the function $\phi(t)$ with the solution obtained for (5).
5: To estimate the parameters of θ by applying the gradient method to (7).
6: To compare the experimental voltage data with the simulated voltage data using the values obtained for θ in the previous step.
7: To validate the model by achieving a relative error of less than 1%.

This law is considered a steepest descent method. The parameter g is a fixed gain called the adaptation gain, and allows the adaptation rate of the parameters to be varied. The initial condition $\hat{\theta}(0)$ is arbitrary, but can be chosen to take into account any a priori knowledge of the plant parameters.

IV. Simulation and Results

The developed algorithm is applied to estimate the ECM parameters for the two databases explained in Section II. To adjust the ECM parameters to the first database, as mentioned in the algorithm, values of the resistors $R_{\mathrm{c}} = 0.1205\ \Omega$ and $R_{\mathrm{a}} = 0.1\ \Omega$ and of the capacitors $C_{\mathrm{c}} = 0.83\ \mu$F and $C_{\mathrm{a}} = 1.25\ \mu$F are used. These values generated $\tau_{\mathrm{c}} = 0.0001$ s, $\tau_{\mathrm{a}} = 0.000125$ s, and the arrays:

$$A = \begin{pmatrix} -10000 & 0 \\ 0 & -8000 \end{pmatrix} \text{ and } B = \begin{pmatrix} 1200 \\ 800 \end{pmatrix}.$$

Thus, using these values of A, B, the input current i_{el} from the first database, and the initial values of the activation voltage $v_{\mathrm{act}}(0) = (v_{\mathrm{act,c}}(0), v_{\mathrm{act,a}}(0)) = (0.255, 0.215)$ V, the solution of (5) is generated. The fourth–order Runge–Kutta iterative method with a step $h = 10^{-7}$ is used to generate the solution of (5). The behavior of the solution given by these values is shown in Figure 7.

Following the algorithm, the function $\phi(t)$ is completed using the obtained values of $v_{\mathrm{act,c}}$ and $v_{\mathrm{act,a}}$. Thus, the parameter vector θ is estimated with the gradient method using $g = 20$ and applying fourth–order Runge–Kutta iterative method with a step of $h = 10^{-7}$ to (7) and (9). It is worth mentioning that the larger the parameter g, the faster the method's convergence speed. However, this implies a smaller step size h and, therefore, greater computational cost. In this case, for $h = 10^{-7}$, the value of $g = 20$ allows the programmed code to run the simulations; that is, the value of g is proposed based on the value of h. The result is $\theta = (4.7454, 0.0477, 0.2774, 0.0530)$ (i.e., $v_{\mathrm{ini}} = 4.7454$ V,

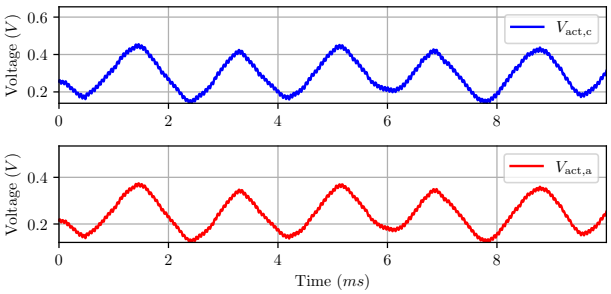

Fig. 7: Behavior of $v_{\mathrm{act,c}}$ and $v_{\mathrm{act,a}}$ as solutions generated by the first input current database, $R_{\mathrm{c}} = 0.1205\ \Omega$, $R_{\mathrm{a}} = 0.1\ \Omega$, $C_{\mathrm{c}} = 0.00083$ F, $C_{\mathrm{a}} = 0.00125$ F, and $v_{\mathrm{act,c}}(0) = 0.255$ V and $v_{\mathrm{act,a}}(0) = 0.215$ V.

$R_{\mathrm{mem}} = 0.0477\ \Omega$, $k_1 = 0.2774$, and $k_2 = 0.0530$). With these parameters and the statistical tests, relative error E_{r}, mean error E_{m}, mean squared error E_{MS}, and root mean squared error E_{RMS} are applied to validate the effectiveness of the ECM. These tests are defined as:

$$E_{\mathrm{r}} = \left(\frac{100}{N_d}\right) \sum_{k=1}^{N_d} \left| \frac{v_{\mathrm{exp,k}} - v_{\mathrm{sim,k}}}{v_{\mathrm{exp,k}}} \right|, \tag{11}$$

$$E_{\mathrm{m}} = \left(\frac{1}{N_d}\right) \sum_{k=1}^{N_d} \left| v_{\mathrm{exp,k}} - v_{\mathrm{sim,k}} \right|, \tag{12}$$

$$E_{\mathrm{MS}} = \left(\frac{1}{N_d}\right) \sum_{k=1}^{N_d} \left(v_{\mathrm{exp,k}} - v_{\mathrm{sim,k}} \right)^2, \tag{13}$$

$$E_{\mathrm{RMS}} = \sqrt{E_{\mathrm{MS}}}, \tag{14}$$

where N_d is the data number. $v_{\mathrm{exp,k}}$ is the k-th voltage data measurement and $v_{\mathrm{sim,k}}$ is the k-th voltage data simulation. The following errors are obtained when compared with the first voltage database, $E_{\mathrm{r}} = 0.5494\%$, $E_{\mathrm{m}} = 0.02726$ V, $E_{\mathrm{MS}} = 0.0012$ V^2, and $E_{\mathrm{RMS}} = 0.0344$ V. Figure 8 shows the simulation result and allows a comparison of real and simulated data. Figure 9 shows a zoom between 3 s and 7 ms to appreciate the accuracy of the simulated curve using the parameters obtained with the proposed algorithm for the first database. To adjust the ECM parameters to the second database, values of the resistors $R_{\mathrm{c}} = 0.024\ \Omega$ and $R_{\mathrm{a}} = 0.024\ \Omega$ and of the capacitors $C_{\mathrm{c}} = 12.5\ \mu F$ and $C_{\mathrm{a}} = 16.7\ \mu F$ are proposed. These values generate $\tau_{\mathrm{c}} = 0.0003\ s$, $\tau_{\mathrm{a}} = 0.0004\ s$, and the arrays:

$$A = \begin{pmatrix} -3000 & 0 \\ 0 & -2400 \end{pmatrix} \text{ and } B = \begin{pmatrix} 80 \\ 60 \end{pmatrix}.$$

Thus, using these values of A, B, the input current i_{el} from the second database, and the initial values $v_{\mathrm{act,c}}(0) = 0.78$ V and $v_{\mathrm{act,a}}(0) = 0.72$ V, the solution of (5) is obtained. The iterative method considers a step $h = 10^{-5}$ to derive a solution of (5). The behavior of the solution using these values is shown in Figure 10. After completion of $\phi(t)$ with

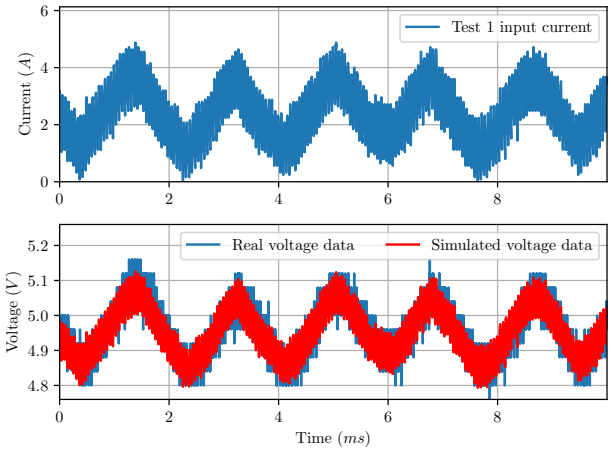

Fig. 8: Comparison between real and simulation voltage data generated by the first input current database.

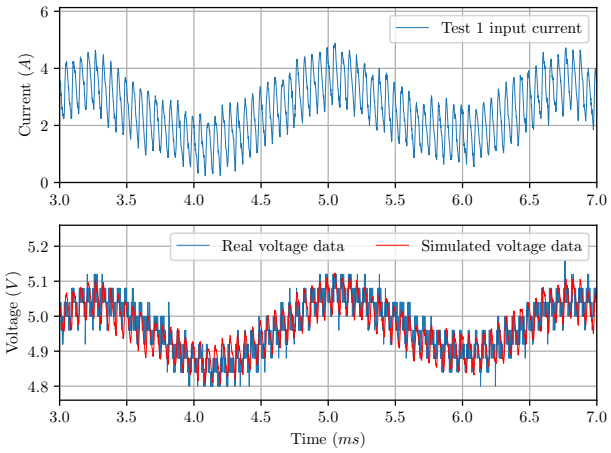

Fig. 9: Zoom for the comparison between real and simulation voltage data generated by the first input current database.

the $v_{\mathrm{act,c}}$ and $v_{\mathrm{act,a}}$ obtained previously, θ is estimated using the gradient method with $g = 20$ and applying fourth–order Runge–Kutta iterative method with a step of $h = 10^{-5}$. The result is $\theta = (7.5240, 0.17911, 0.1639, 0.0251)$ (i.e., $v_{\mathrm{ini}} = 7.5240$ V, $R_{\mathrm{mem}} = 0.1791\ \Omega$, $k_1 = 0.1639$, and $k_2 = 0.0251$). The errors $E_{\mathrm{r}} = 0.8997\%$, $E_{\mathrm{m}} = 0.0792$ V, $E_{\mathrm{MS}} = 0.0090$ V^2, and $E_{\mathrm{RMS}} = 0.0952$ V are obtained as a result of the comparison between the simulation performed with this θ and the second voltage database. Figure 11 shows the simulation result and allows a comparison of real and simulated data. Figure 12 shows a zoom between 20 ms and 30 ms to appreciate the accuracy of the simulated curve using the parameters obtained with the proposed algorithm for the second database.

As can be seen, the calculated parameters for the ECM using the developed algorithm allow obtaining a performance greater than 99% for both databases. This demonstrates the efficiency of the proposed algorithm.

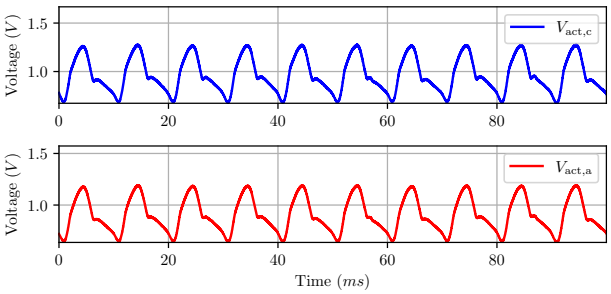

Fig. 10: Behavior of $v_{\mathrm{act,c}}$ and $v_{\mathrm{act,a}}$ as solutions generated by the second input current database, $R_{\mathrm{c}} = 0.024\ \Omega$, $R_{\mathrm{a}} = 0.024\ \Omega$, $C_{\mathrm{c}} = 0.0125$ F, $C_{\mathrm{a}} = 0.0167$ F, and $v_{\mathrm{act,c}}(0) = 0.78$ V and $v_{\mathrm{act,a}}(0) = 0.72$ V.

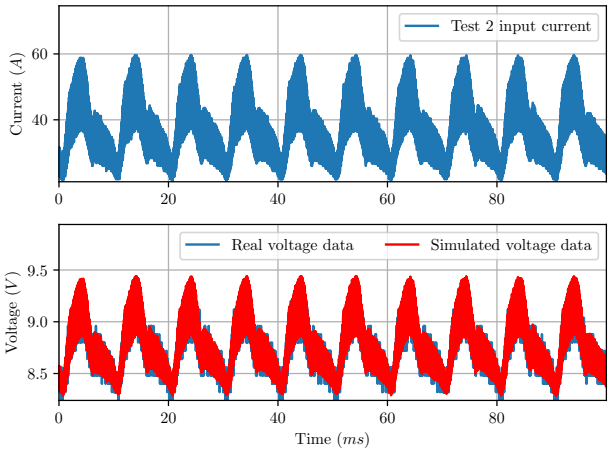

Fig. 11: Comparison between real and simulation voltage data generated by the second input current database.

A. Discussion

The algorithm detailed in this work allows for calculating the parameters of an ECM depending on the values suggested for the electrical components (resistors and capacitors). The results of the different statistical tests show the performance of the algorithm for two databases. Table II presents a comparison of the proposed algorithm with the multi-innovation least squares (MILS) algorithm developed in [15], which is the only one reported to estimate ECM parameters for the PEM electrolyzer voltage. This comparison takes into account the two parameters of innovation length (p) with the highest reported performance in [15], $p = 4$ and $p = 5$. As can be seen in Table II, the amount of data used to validate the algorithm is double and the relative error obtained for the estimated parameters in both databases is lower than that reported using the MILS algorithm. However, the time to obtain the estimated parameters is considerably longer. Therefore, the proposed algorithm offers greater accuracy in exchange for a greater amount of time and iterations.

Different values of the resistors and capacitors allow finding parameters with non-significant errors for the two databases,

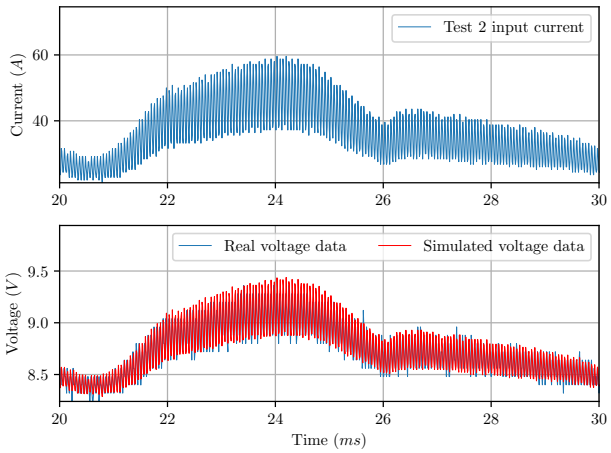

Fig. 12: Zoom for the comparison between real and simulation voltage data generated by the second input current database.

TABLE II: Comparison of the proposed algorithm with the reported MILS algorithm for $p = 4, 5$ in [15].

Algorithm	Data points	E_r	Time
MILS ($p = 4$)	5000	3.07%	10 s
MILS ($p = 5$)	5000	1.30%	10 s
Proposed (Database 1)	10000	0.5494%	133 s
Proposed (Database 2)	10000	0.8997%	2209 s

which demonstrates the versatility of the proposed algorithm. For example, for database 1, using resistor values $R_c = 0.48$ Ω and $R_a = 0.4$ Ω and capacitor values $C_c = 416.7$ μF and $C_a = 625$ μF the values $\tau_c = 0.2$ s, $\tau_a = 0.25$ s, A, and B are obtained, where

$$A = \begin{pmatrix} -5 & 0 \\ 0 & -4 \end{pmatrix} \text{ and } B = \begin{pmatrix} 2.4 \\ 1.6 \end{pmatrix}.$$

Besides, with the initial values $v_{act,c}(0) = 1.22$ V and $v_{act,a}(0) = 1.1$ V, it is possible to obtain $\theta = (4.6498, 0.0315, 0.0946, 0.1221)$ or $v_{ini} = 4.6498$ V, $R_{mem} = 0.0315$ Ω, $k_1 = 0.0946$, and $k_2 = 0.1221$. With this value of θ, the errors were $E_r = 0.4998\%$, $E_m = 0.0248$ V, $E_{MS} = 0.0010$ V^2, and $E_{RMS} = 0.0311$ V. For database 2, one example is given using resistor values $R_c = 0.0301$ Ω and $R_a = 0.024$ Ω and capacitor values $C_c = 8.3$ μF and $C_a = 12.5$ μ F. Thus, the values $\tau_c = 0.00025$ s, $\tau_a = 0.0003$ s, A and B are obtained, where

$$A = \begin{pmatrix} -4000 & 0 \\ 0 & -3200 \end{pmatrix} \text{ and } B = \begin{pmatrix} 120 \\ 80 \end{pmatrix}.$$

Besides, $\theta = (7.4014, 0.0238, -0.0071, 0.5827)$ or $v_{ini} = 7.4014$ V, $R_{mem} = 0.0238\,\Omega$, $k_1 = -0.0071$, and $k_2 = 0.5827$ are obtained with the initial values $v_{act,c}(0) = 1$ V and $v_{act,a}(0) = 1$ V. Using these parameters, the errors are $E_r = 0.9999\%$, $E_m = 0.0881$ V, $E_{MS} = 0.0118$ V^2, and $E_{RMS} = 0.1087$ V. Furthermore, the proposed algorithm allows for estimating the ECM parameters for each operating point of the PEM electrolyzer, which usually works at a fixed nominal point. However, parameters estimated for one database may not be able to be efficiently estimated for another database, which can be considered a disadvantage of the proposed algorithm.

TABLE III: Algorithm performance measurements for the two databases.

Database	E_r for initial iteration	Iterations	E_r for final iteration	Time
1	11.0248%	43	0.9822%	59 s
1	6.2930%	95	0.9977%	139 s
1	17.8114%	94	0.9981%	136 s
2	105.1289%	2717	0.9999%	3131 s
2	43.5527%	1636	0.9999%	1867 s
2	2.8383%	612	0.9994%	714 s

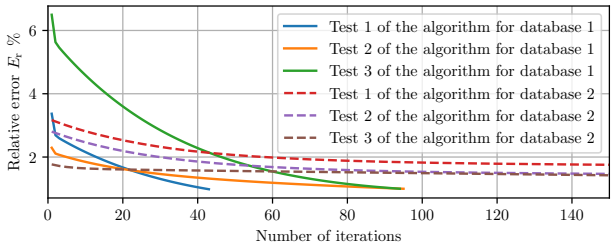

Fig. 13: Relative error behavior for the algorithm iterations when applied to different initial parameters to estimate the parameters of the ECM for the two databases.

To appreciate the proposed algorithm's performance measurements of the number of iterations, the convergence time, and the relative error were taken during its application using different initial parameter values and $g = 40$, see Table III. The initial parameters varied, for the first database, between 0.1 and 0.2 ms for τ_c; between 0.06 and 0.12 ms for τ_a; between 0.71 and 1.25 mF for C_c; between 1.25 and 3.33 mF for C_a; between 4.2 and 5.2 V for V_{ini}; between 0.15 and 0.47 Ω for R_{mem}; between 0.13 and 0.27 for k_1; between 0.01 and 0.05 for k_2. For the second database, between 0.25 and 0.5 ms for τ_c; between 0.33 and 1 ms for τ_a; between 0.62 and 0.83 mF for C_c; between 1.25 and 2.5 mF for C_a; between 7 and 8.5 V for V_{ini}; between 0.15 and 0.28 Ω for R_{mem}; between 0.1 and 0.15 for k_1; between 0.0351 and 0.251 for k_2. The initial values for V_{act} generation were constant depending on the database, for the first one $V_{act}(0) = (0.255, 0.215)$ V and for the second one $V_{act}(0) = (0.78, 0.72)$ V.

As can be seen in Table III and Figure 13, when using different initial parameter values, the number of iterations and the convergence rate for a relative error of less than 1% is much lower for the first database than the second database using the proposed algorithm. This is due to the complexity of the signals obtained from the second database. For this reason, when the program runs for a certain amount of time, the errors obtained for the simulations of the first database are smaller than the errors obtained for the simulations of the second database. Furthermore, based on Table III, the approximate computation time per iteration is 1.25 seconds using a code programmed in Python programming language (Python version: 3.8.10 for 64 bits).

V. Conclusion

In this work, an algorithm to estimate the parameters of an ECM for the PEM electrolyzer voltage is detailed and validated. The proposed algorithm allows for adjusting the parameters based on the values of the electronic components. Besides, the algorithm is explained in detail to facilitate the calculation of the ECM parameters. Furthermore, this innovative algorithm is important for the design and construction of an emulator modeling the PEM electrolyzer voltage response under current ripple constraints. This work will lead to further investigations into the current ripple (amplitude, frequency, and waveform) that occur in a PEM electrolyzer. Furthermore, current research work is towards the online computation of the proposed algorithm for feedback purposes.

VI. Acknowledgment

The authors would like to thank the Consejo Nacional de Humanidades, Ciencias y Tecnologías (CONAHCYT) Mexico for the program Posdoctoral Stays in Mexico 2022 (1) in the Modality Academic Postdoctoral Stay 2022 (1).

References

[1] N. Lazaar, M. Barakat, M. Hafiane, J. Sabor, and H. Gualous, "Modeling and control of a hydrogen-based green data center," *Electric Power Systems Research*, vol. 199, p. 107374, 2021.

[2] G. De Carne, S. M. Maroufi, H. Beiranvand, V. De Angelis, S. D'Arco, V. Gevorgian, S. Waczowicz, B. Mather, M. Liserre, and V. Hagenmeyer, "The role of energy storage systems for a secure energy supply: A comprehensive review of system needs and technology solutions," *Electric Power Systems Research*, vol. 236, p. 110963, 2024.

[3] J. Ramsebner, P. Linares, A. Hiesl, and R. Haas, "Techno-economic evaluation of renewable hydrogen generation strategies for the industrial sector," *International Journal of Hydrogen Energy*, vol. 60, pp. 1020–1040, 2024. [Online]. Available: https://www.sciencedirect.com/science/article/pii/S0360319924005871

[4] H. Sayed-Ahmed, A. Toldy, and A. Santasalo-Aarnio, "Dynamic operation of proton exchange membrane electrolyzers—critical review," *Renewable and Sustainable Energy Reviews*, vol. 189, p. 113883, 2024. [Online]. Available: https://www.sciencedirect.com/science/article/pii/S1364032123007414

[5] R. Cozzolino and G. Bella, "A review of electrolyzer-based systems providing grid ancillary services: current status, market, challenges and future directions," *Frontiers in Energy Research*, vol. 12, 2024. [Online]. Available: https://www.frontiersin.org/articles/10.3389/fenrg.2024.1358333

[6] E. K. Volk, M. E. Kreider, S. Kwon, and S. M. Alia, "Recent progress in understanding the catalyst layer in anion exchange membrane electrolyzers – durability, utilization, and integration," *EES Catalysis*, vol. 2, no. 1, pp. 109–137, 2024. [Online]. Available: https://www.sciencedirect.com/science/article/pii/S2753801X24000119

[7] S. Krishnan, V. Koning, M. Theodorus de Groot, A. de Groot, P. G. Mendoza, M. Junginger, and G. J. Kramer, "Present and future cost of alkaline and pem electrolyser stacks," *International Journal of Hydrogen Energy*, vol. 48, no. 83, pp. 32 313–32 330, 2023. [Online]. Available: https://www.sciencedirect.com/science/article/pii/S0360319923022590

[8] N. Dubouis, D. Aymé-Perrot, D. Degoulange, A. Grimaud, and H. Girault, "Alkaline electrolyzers: Powering industries and overcoming fundamental challenges," *Joule*, 2024. [Online]. Available: https://www.sciencedirect.com/science/article/pii/S2542435124000953

[9] M. Mittenbühler, J. Zhang, and A. Benigni, "Automatically optimized component model computation for power system simulation on gpu," *Electric Power Systems Research*, vol. 235, p. 110740, 2024.

[10] D. Falcão and A. Pinto, "A review on pem electrolyzer modelling: Guidelines for beginners," *Journal of Cleaner Production*, vol. 261, p. 121184, 2020.

[11] A. Hernández-Gómez, V. Ramirez, and D. Guilbert, "Investigation of pem electrolyzer modeling: Electrical domain, efficiency, and specific energy consumption," *International Journal of Hydrogen Energy*, vol. 45, no. 29, pp. 14 625–14 639, 2020.

[12] M. Koundi, H. E. Fadil, Z. E. Idrissi, A. Lassioui, T. Bouanou, S. Nady, A. Rachid, and A. Hilmani, "Electrical modelling, design, and implementation of a hardware pem electrolyzer emulator for smart grid testing," *International Journal of Emerging Electric Power Systems*, 2024. [Online]. Available: https://doi.org/10.1515/ijeeps-2023-0213

[13] F. Parache, H. Schneider, C. Turpin, N. Richet, O. Debellemaniére, E. Bru, A. T. Thieu, C. Bertail, and C. Marot, "Impact of power converter current ripple on the degradation of pem electrolyzer performances," *Membranes*, vol. 12, no. 2, 2022. [Online]. Available: https://www.mdpi.com/2077-0375/12/2/109

[14] D. Yousri, H. E. Z. Farag, H. Zeineldin, and E. F. El-Saadany, "Optimal electrochemical model parameters identification for utility-scale pem electrolyzers," in *2024 IEEE Power & Energy Society General Meeting (PESGM)*, 2024, pp. 1–5.

[15] X. Mao, Y. Tian, A. Yang, and G. Zhang, "Identification of equivalent circuit parameters for proton exchange membrane (pem) electrolyzer engineering models," *IEEE Access*, vol. 12, pp. 15 509–15 524, 2024.

[16] S. Toghyani, S. Fakhradini, E. Afshari, E. Baniasadi, M. Y. Abdollahzadeh Jamalabadi, and M. Safdari Shadloo, "Optimization of operating parameters of a polymer exchange membrane electrolyzer," *International Journal of Hydrogen Energy*, vol. 44, no. 13, pp. 6403–6414, 2019.

[17] R. Khajuria, R. Lamba, and R. Kumar, "Model parameter extraction for pem electrolyzer using honey badger algorithm," in *2023 IEEE 3rd International Conference on Sustainable Energy and Future Electric Transportation (SEFET)*, 2023, pp. 1–6.

[18] R. Khajuria, S. Yelisetti, R. Lamba, and R. Kumar, "Optimal model parameter estimation and performance analysis of pem electrolyzer using modified honey badger algorithm," *International Journal of Hydrogen Energy*, vol. 49, pp. 238–259, 2024.

[19] M. A. Aftab, V. C. Pandey, S. G. Krishnan, F. Mir, G. Rolofs, E. Chukwureh, S. Ahmed, and C. Konstantinou, "Demand flexibility in hydrogen production by incorporating electrical and physical parameters," *Electric Power Systems Research*, vol. 239, p. 111213, 2025.

[20] J. Zhang, F. Xiao, F. Ma, L. Sun, Y. Zhang, and R. Xiao, "Capacity optimization allocation method for off-grid res-h2 microgrid system considering the load-follow-source mechanism," *Electric Power Systems Research*, vol. 231, p. 110378, 2024.

[21] H. Nezhadkhatami, A. Hajizadeh, M. Soltani, and D. Guilbert, "Variant parameters identification of the pemel circuit model by rmse-based self-tuning method," in *2023 IEEE 32nd International Symposium on Industrial Electronics (ISIE)*, 2023, pp. 1–6.

[22] G. Fontès, C. Turpin, R. Saisset, T. A. Meynard, and S. Astier, "Interactions between fuel cells and power converters: Influence of current harmonics on a fuel cell stack," *IEEE Transactions on Power Electronics*, vol. 22, pp. 670–678, 2007. [Online]. Available: https://api.semanticscholar.org/CorpusID:25098644

[23] B. Yodwong, D. Guilbert, M. Phattanasak, W. Kaewmanee, M. Hinaje, and G. Vitale, "Proton exchange membrane electrolyzer modeling for power electronics control: A short review," *C*, vol. 6, no. 2, 2020.

[24] Z. Lukács and T. Kristóf, "A generalized model of the equivalent circuits in the electrochemical impedance spectroscopy," *Electrochimica Acta*, vol. 363, p. 137199, 2020.

[25] C.-T. Pham and D. Månsson, "On the physical system modelling of energy storages as equivalent circuits with parameter description for variable load demand (part i)," *Journal of Energy Storage*, vol. 13, pp. 73–84, 2017.

[26] A. Hernández-Gómez, V. Ramirez, D. Guilbert, and B. Saldivar, "Cell voltage static-dynamic modeling of a pem electrolyzer based on adaptive parameters: Development and experimental validation," *Renewable Energy*, vol. 163, pp. 1508–1522, 2021.

[27] ——, "Development of an adaptive static-dynamic electrical model based on input electrical energy for pem water electrolysis," *International Journal of Hydrogen Energy*, vol. 45, no. 38, pp. 18 817–18 830, 2020.

[28] S. Sastry and M. Bodson, *Adaptive Control: Stability, Convergence and Robustness*, ser. Dover Books on Electrical Engineering Series. Dover Publications, 2011. [Online]. Available: https://books.google.com.mx/books?id=-cOviBa9pR8C